Article ID: 1007-4627(2012)01-0014-07

Momentum Distribution of Nucleons in Asymmetric Nuclear Matter

LI Jian-yang[1,2], ZUO Wei[1,2], CAO Gao-qing[1,2], U. Lombardo[3]

(1. *Institute of Modern Physics, Chinese Academy of Sciences, Lanzhou* 730000, *China*;
2. *Graduate University of Chinese Academy of Sciences, Beijing* 100049, *China*;
3. *Department of Physics and Astrophysics, Catania University, Via Santa Sofia* 64, *I*-95123, *and INFN-LNS, Via Santa Sofia* 44, *I*-95123 *Catania, Italy*)

Abstract: We calculate the momentum distribution of nucleons in asymmetric nuclear matter within the framework of the extended Brueckner-Hartree-Fock approximation at zero temperature, use Argonne V18 potential as two nucleons potential. The isospin-asymmetry dependence of the nucleon momentum distribution predicted and discussed. It is shown that as the asymmetry increases, the proton momentum distribution become smaller while the neutron one gets higher below their respective Fermi surfaces with respect to their common values in symmetric nuclear matter. The quasi-particle strength at the Fermi momentum also calculated and discussed, we got an improved fulfillment of the Migdal-Luttinger theorem and nucleon number conservation.

Key words: asymmetric nuclear matter; Brueckner theory; momentum distribution; quasi-particle strength

CLC number: O571.22 **Document code**: A

1 Introduction

Many-body correlations induced by the nucleon-nucleon interactions among nucleons play an important role in a nuclear many-body system, which make the system much more complicated and have more plentiful properties than a non-interacting Fermi system. For example, the effect of correlations leads to the depletion of the nucleon momentum distribution below the Fermi momentum and the population above the Fermi momentum in nuclear matter[1-2]. In nuclear matter the stationary states are plane waves, so that the occupation probability for the "orbit" $|k\rangle$ is given by the momentum distribution $n(k)$. The momentum distribution of nucleons in nuclear matter has been investigated extensively by using various theoretical methods and models[2-7]. The related experimental data are also reported continually[8-11]. The nucleon momentum distribution is of great physical interest since it can be related to experiment observables in pick-up and knock-out reactions[6]. In Ref. [6], the authors calculated the nucleon momentum distribution and quasi-particle strength in symmetric nuclear matter in the framework of the

Received Date: 22 Feb. 2011; **Revised date**: 26 Feb. 2011

Foundation item: National Natural Science Foundation of China(10875151, 10740420550); Knowledge Innovation Project of Chinese Academy of Sciences(KJCX3-SYW-N2); Major State Basic Research Development Program of China(2007CB15004); Chinese Academy of Sciences Visiting Professorship for Senior International Scientists(2009J2-26); CAS/SAFEA International Partnership Program for Creative Research Teams(CXTD-J2005-1)

Biography: LI Jian-yang (1985—), Male, Ningxia, Master, working on particle physics and nuclear physics;
E-mail: lijianyang@impcas.ac.cn

Corresponding author: ZUO Wei, E-mail: zuowei@impcas.ac.cn

Brueckner-Bethe-Goldstone theory by including high-order contributions in the hole-line expansion of the mass operator and they found a good agreement between their calculated results and the experimental data. In the present paper, we shall extend the previous investigation of Ref. [6] to asymmetric nuclear matter and investigate the isospin dependence of the nucleon momentum distribution within the extended Brueckner-Hartree-Fock (EBHF). We improve the previous calculation by including the renormalization contributions in the hole-line expansion of the mass operator and got an improved fulfillment of the Migdal-Lut- tinger theorem. The quasi-particle strength is also predicted and the resulting value turns out to be in good agreement with experimental data[4, 8].

The present paper is organized as follows. We will describe briefly the adopted theoretical approach in Section 2. The numerical results are presented and discussed in Section 3. In Section 4 a summary is presented.

2 Theoretical framework

The present studies are based on the EBHF approach for asymmetric nuclear matter[12]. The starting point of this framework is Brueckner reaction G matrix which satisfies the following Bethe-Goldstone (BG) equation[1]

$$G(\rho,\ \beta;\ \omega)=v_{\mathrm{NN}}+v_{\mathrm{NN}}\sum_{k_1k_2}\frac{|k_1k_2\rangle Q(k_1,\ k_2)\langle k_1k_2|}{\omega-\varepsilon(k_1)-\varepsilon(k_2)+\mathrm{i}\eta}G(\rho,\ \beta;\ \omega)\ , \quad (1)$$

where v_{NN} is the realistic nucleon-nucleon interaction, and we adopt the Argonne V18 two-body interaction[13] in our present calculation. In Ref. [11] it has been shown that three-body forces have very little influence on the nucleon momentum distribution[11] and thus we do not include three-body effect in the present calculations. $Q(k_1,\ k_2)$ is the Pauli operator which prevents the two intermediate nucleons from being scattered into the states below the Fermi sea. The isospin asymmetry parameter is defined as $\beta=(\rho_{\mathrm{n}}-\rho_{\mathrm{p}})/\rho$, where ρ_{n}, ρ_{p} and ρ denote the neutron, proton and total nucleon number densities, respectively. The BHF single particle (s. p.) energy is given by

$$\varepsilon(k)=\frac{\hbar^2k^2}{2m}+U_1(k)\ .$$

In solving the BG equation for the G-matrix, we adopt the continuous choice for the s. p. potential U_1. Under the continuous choice, the s. p. potential describes physically at the lowest BHF level the nuclear mean field felt by a nucleon in nuclear medium and is calculated from the real part of the on-shell G-matrix, i. e.,

$$U_1(k)=\sum_{k'}n(k')\times \mathrm{Re}\langle kk'|G[\varepsilon(k)+\varepsilon(k')]|kk'\rangle_A\ ,$$

as pointed out by Mahaux et al.[1]. In order to predict reliably the s. p. properties within the Brueckner theory, one has to go beyond the lowest BHF approximation by considering the high-order contributions in the hole-line expansion of the mass operator. The mass operator is defined as[1],

$$M(k,\ \omega)=V(k,\ \omega)+\mathrm{i}W(k,\ \omega)\ , \quad (2)$$

which is a complex quantity and its on-shell value can be identified with the potential energy felt by a nucleon in nuclear matter. According to the Brueckner-Bethe-Goldstone theory, the mass operator can be expanded in a perturbation series according to the number of hole lines, i. e.,

$$M(k,\ \omega)=M_1(k,\ \omega)+M_2(k,\ \omega)+M_3(k,\ \omega)+\cdots\ . \quad (3)$$

The sum of all one-hole line graphs is called the BHF approximation to the mass operator, it reads,

$$M_1(k,\ \omega)=\sum_j n_<(j)\langle k,\ j|G[\omega+\varepsilon(j)]|k,\ j\rangle_A. \quad (4)$$

Hereafter, we shall use j, l, $\cdots$ denote the s. p. states below the Fermi momentum; a, b, $\cdots$ denote the states above the Fermi momentum; and k denote the s. p. states of both cases.

$$n_<(k)=1-n_>(k)=\theta(k_F-k)$$

is the momentum distribution in the uncorrelated ground state and the index "A" refers to the anti-symmetrization of the product of two plane waves. The on-shell value of the lowest-order contribution $M_1(k,\omega)$ corresponds to the BHF s. p. potential $U_1(k)$. The second order term M_2 is the so-called rearrangement contribution. It stems from the medium dependence of the G matrix via the Pauli operator in the BG equation which plays an important role for satisfactorily reproducing the depth of the empirical nuclear optical potential and crucial for restoring the Hugenholtz-Van Hove theorem[1, 12]. The expression of M_2 reads,

$$M_2(k,\omega)=\frac{1}{2}\sum_{j,l,a} n_<(j)n_<(l)n_>(a)\times \frac{|\langle j,l|G[\varepsilon(j)+\varepsilon(l)]|k,a\rangle_A|^2}{\omega+\varepsilon(a)-\varepsilon(j)-\varepsilon(l)-i\eta}. \quad (5)$$

Due to many-body correlations, the Fermi seas in asymmetric nuclear matter are partially depleted, and thus the correlated momentum distributions differ from the uncorrelated ones. To account for this physical effect, we consider the third-order term M_3 in the hole-line expansion of the mass operator. M_3 is the renormalization contribution to the BHF mass operator M_1 and it reads[4],

$$M_3(k,\omega)=-\sum_j \kappa_2(j)\times \langle k,j|G[\omega+\varepsilon(j)]|k,j\rangle_A, \quad (6)$$

where

$$\kappa_2(j)=-\left[\frac{\partial M_1(j,\omega)}{\partial\omega}\right]_{\omega=\varepsilon(j)} \quad (7)$$

is at the lowest-order the depletion of neutron or proton Fermi sea[1, 12]. By considering the sum of M_1 and M_3, one gets a renormalized BHF approximation for the mass operator, i. e.,

$$\begin{aligned}\tilde{M}_1(k,\omega)&\equiv M_1(k,\omega)+M_3(k,\omega)\\&=\sum_j[1-\kappa_2(j)]\langle k,j|G[\omega+\varepsilon(j)]|k,j\rangle_A\\&=\sum_j n_2(j)\langle k,j|G[\omega+\varepsilon(j)]|k,j\rangle_A, \end{aligned}\quad (8)$$

here $n_2(j)$ is the second-order approximation to the momentum distribution in the correlated ground state ($j<k_F$), it reads

$$n_2(k)=1+\left[\frac{\partial M_1(k,\omega)}{\partial\omega}\right]_{\omega=\varepsilon(k)}, \text{ for } k<k_F. \quad (9)$$

Including the renormalization contribution to M_1, one gets the following momentum distribution below the Fermi surface (see Eq. (2.192) of Ref. [1]),

$$\tilde{n}_2(k)=1+\left[\frac{\partial M_1(k,\omega)}{\partial\omega}+\frac{\partial M_3(k,\omega)}{\partial\omega}\right]_{\omega=\varepsilon(k)}, \text{ for } k<k_F. \quad (10)$$

As shown in Ref. [4], it is a very accurate approximation to replace in Eq. (6) the coefficient $\kappa_2(j)$ by its value κ at the average of j in the Fermi sea, i. e., at $j=0.75k_F$. We have,

$$M_3(k,\omega)\approx-\kappa M_1(k,\omega), \quad (11)$$

where $\kappa=[1-n_2(j)]_{j=0.75k_F}$. Similarly, we can get the momentum distribution above the Fermi surface (see Eq. (2.196) of Ref. [1]), i. e.,

$$\begin{aligned}\tilde{n}_2(k)&=-\left[\frac{\partial M_2(k,\omega)}{\partial\omega}+\frac{\partial M_4(k,\omega)}{\partial\omega}\right]_{\omega=\varepsilon(k)}\\&\approx-(1-\kappa)\left[\frac{\partial M_2(k,\omega)}{\partial\omega}\right]_{\omega=\varepsilon(k)}, \ k>k_F. \end{aligned}\quad (12)$$

The quasi-particle strength is defined by following expression

$$Z(k)=\left\{1-\frac{\partial}{\partial\omega}\mathrm{Re}\,[M(k,\omega)]\right\}^{-1}_{\omega=\varepsilon(k)}. \quad (13)$$

Up to second order approximation, it can be written as[6],

$$Z(k)=\left\{1-\frac{\partial}{\partial\omega}\mathrm{Re}\,[M_1(k,\omega)+M_2(k,\omega)]\right\}^{-1}_{\omega=\varepsilon(k)}. \quad (14)$$

According to the argument of Ref. [14], higher-order contributions are strongly cancelled with each other, and thus the above approximation is of good accuracy.

According to Migdal-Luttinger theorem, the discontinuity of momentum distribution at Fermi

momentum k_F should equal to the quasi-particle strength at k_F, this property together with particle number conservation are used as criteria to assess the validity of the theoretical methods for calculating the momentum distribution[15]. The fulfillment of particle number conservation reads[4]

$$\frac{3}{k_F^3}\int_0^\infty \tilde{n}_2(k)k^2\,\mathrm{d}k = 1\ . \tag{15}$$

3 Results and discussions

In this section we shall show the calculated momentum distribution of asymmetric nuclear matter at various densities and isospin-asymmetries.

In Fig. 1 we display the renormalization effects on the predicted momentum distribution $n(k)$, i. e., the effects induced by the third-order term M_3 and the fourth-order term M_4 in the hole-line expansion of the mass operator. From the Fig. 1,

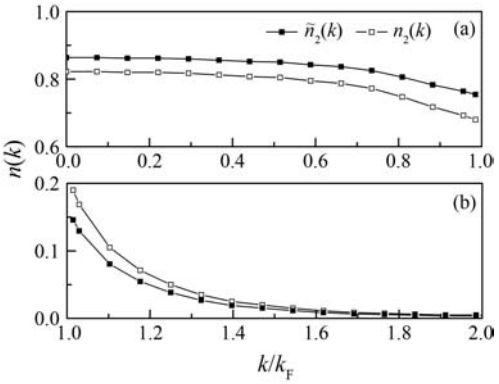

Fig. 1 Momentum distribution below (a) and above (b) the Fermi surface in symmetric nuclear matter at $k_F = 1.36$ fm^{-1}. The open squares $n_2(k)$ are obtained in the case of not considering the renormalization contributions and the solid squares $\tilde{n}_2(k)$ show the results by including the renormalization effects.

one can see that due to the many-body correlations, the s. p. states under the Fermi surface are partly emptied, and those above the Fermi surface are partly occupied in the ground state of nuclear matter. The horizontal axis is the ratio of momentum of nucleon state to Fermi momentum, and vertical axis is the occupation probability for the nucleons state $|k\rangle$. The open squares $n_2(k)$ are obtained in the case of not considering the renormalization contributions and the solid squares $\tilde{n}_2(k)$ show the results by including the renormalization effects.

By comparing the solid squares and the corresponding open squares, it is noticed that the renormalization terms in the hole-line expansion of the mass operator yields a non-negligible contribution on the nucleon momentum distribution.

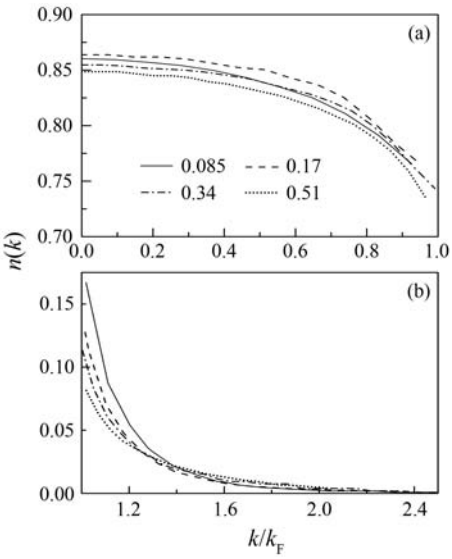

Fig. 2 Nucleon momentum distribution in symmetric nuclear matter at four density values $\rho = 0.085$, 0.17, 0.34 and 0.51 fm^{-3}.
(a) for momentum smaller than their respectively Fermi momentum and (b) for momentum larger than their respective Fermi momentum.

It turns out under the Fermi surface, when including the renormalization effect, occupation probability of nucleons is getting larger while above the Fermi surface, the occupation probability is getting smaller, and this renormalization effect should remain satisfied with the nucleons sum rule. Our results are in fairly good agreement with those obtained in Ref. [6] where the author adopted a different scheme to account for higher-order contributions instead of considering the renormalization terms.

In the following, all momentum distributions

are calculated by including the renormalization effects. In Fig. 2 we show $n(k)$ in symmetric nuclear matter at four different density values $\rho=0.085$, 0.17, 0.34 and 0.51 fm^{-3}. It is seen that the density dependence of the momentum distribution, as a function of the ratio k/k_F, is quite weak, which is consistent with the EBHF calculation in Ref. [6] by adopting the separable AV14 interaction and the prediction reported in Ref. [7] by using the Green Function method.

In Fig. 3, we report the neutron and proton momentum distributions below their respective Fermi surfaces in asymmetry nuclear matter at various asymmetries $\beta=0$, 0.2, 0.4, 0.6, 0.8 for two densities $\rho=0.17$ and 0.34 fm^{-3}. In Fig. 4, the corresponding results of the momentum distributions above the Fermi surface are plotted . We

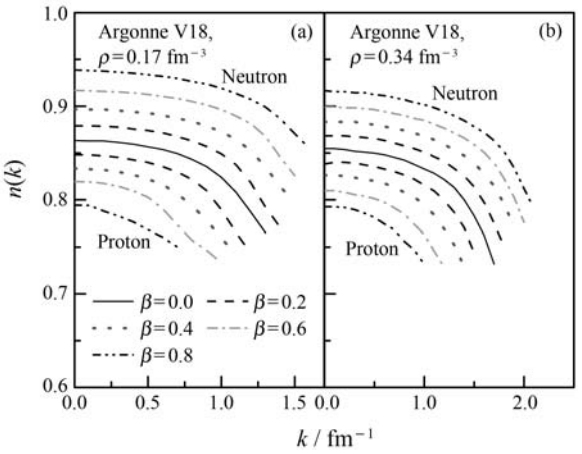

Fig. 3 Neutron and proton momentum distributions below their respective Fermi surfaces in asymmetric nuclear matter at various asymmetry parameters.

see that above Fermi surface, at various asymmetry parameters, momentum distributions of neutrons are nearly overlapped. This may due to the fact that some parameters we choose in our calculation are not of precision. At the density $\rho=0.34$ fm^{-3}, the curve at large momentums shows slightly vibration, this may be caused by the instability in the calculations at large momentums and high densities. As an *ab initio* description, we accept these results. It is clearly seen that the momentum distributions of protons and neutrons depend sensitively on the isospin-asymmetry. As the asymmetry increases, the momentum distribution of protons becomes lower while neutrons one gets higher below their respective Fermi surfaces with respect to their common values in symmetric nuclear matter, namely, as increase of asymmetry parameter, the neutron depletion below its Fermi momentum becomes smaller, while the proton depletion below its Fermi momentum becomes larger. Such an isospin-asymmetry dependence of the neutron and proton momentum distributions implies that at a higher asymmetry, the many-body correlations induced by the nucleon-nucleon interaction becomes stronger on protons and weaker on neutrons.

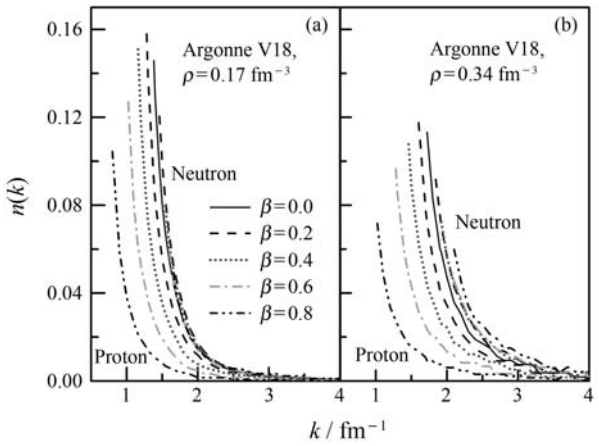

Fig. 4 Neutron and proton momentum distributions above their respective Fermi surfaces in asymmetric nuclear matter at various asymmetry parameters.

In order to see more clearly the isospin dependence, in Fig. 5 we display the occupation probability of proton and neutron at momentum $k=0$ as functions of the isospin-asymmetry. One may notice from the figure that the neutron momentum distribution $n_n(k=0)$ increases and the proton one $n_p(k=0)$ decreases almost linearly as increasing asymmetry. This is consistent with prediction reported in Ref. [7] by using the Green Function method.

As a criterion to assess our calculation, we have calculated the left hand side of the sum rule of Eq. (15), and the integration is carried out up to

4.0 fm^{-1} for $\rho=0.17$ fm^{-3}. The results are given in Table 1.

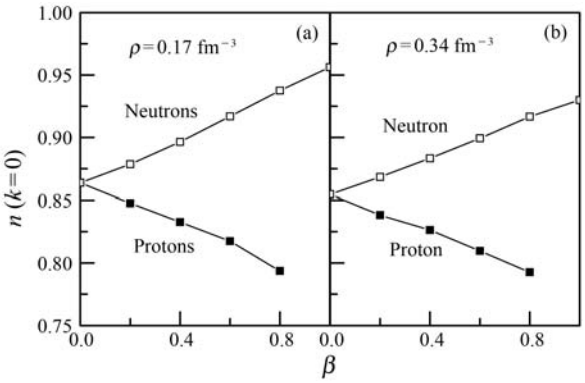

Fig. 5 The neutron and proton momentum distribution at $k=0$ in asymmetry nuclear matter vs. isospin asymmetry.

Table 1 Nucleon number conservation of asymmetry nuclear matter at density $\rho=0.17$ fm^{-3}

β	Proton sum	Neutron sum
0.0	0.98	0.98
0.2	0.99	0.99
0.4	0.99	0.98
0.6	0.98	0.95
0.8	0.98	0.99

It is seen that the particle number conservation is fulfilled satisfactorily in our improved approximation.

According to the Migdal-Luttinger theorem, at Fermi momentum k_F, the quasi-particle strength defined in Eq. (13) must be equal to the discontinuity of the momentum distribution at the Fermi momentum. In our approximation scheme [see Eqs. (10) and (12)], the discontinuity at k_F can be written

$$\tilde{Z}(k_F)=\tilde{n}_2(k_F^-)-\tilde{n}_2(k_F^+)\ . \qquad (16)$$

We have calculated the two quantities for symmetry nuclear matter at $\rho=0.17$ fm^{-3}, and obtained $\tilde{Z}(k_F)=0.61$ and $Z(k_F)=0.64$. This means that the Migdal-Luttinger theorem is violated only by about 4.7% in our calculation and the fulfillment of the Migdal-Luttinger theorem is better than that in Ref. [6] where the authors got $\tilde{Z}=0.56$, $Z(k_F)=0.64$, and the theorem is violated by 12.5%. The above-obtained satisfactory fulfillment of the nucleon number conservation and the Migdal-Luttinger theorem indicates that our present calculations are quite reliable.

We have also calculated quasi-particle strength and the discontinuity of the momentum distribution at Fermi momentum k_F in asymmetric nuclear matter at various asymmetries for two densities $\rho=0.17$, 0.34 fm^{-3}. The results are shown separately in Tables 2 and 3. By comparing the two tables, we see that the Migdal-Luttinger theorem is fulfilled satisfactorily in our approximation for all asymmetries considered.

Table 2 Quasi-particle strength calculated in Eq. (14), for two densities and at various asymmetry parameters

β	$\rho=0.17$ fm^{-3}		$\rho=0.34$ fm^{-3}	
	Neutron	Proton	Neutron	Proton
0.0	0.64	0.64	0.66	0.66
0.2	0.61	0.68	0.65	0.69
0.4	0.61	0.73	0.63	0.72
0.6	0.61	0.78	0.63	0.74
0.8	0.62	0.81	0.64	0.75

Table 3 Discontinuity of the momentum distribution at Fermi momentum, calculated in Eq. (16), for two densities and at various asymmetry parameters

β	$\rho=0.17$ fm^{-3}		$\rho=0.34$ fm^{-3}	
	Neutron	Proton	Neutron	Proton
0.0	0.61	0.61	0.62	0.62
0.2	0.58	0.65	0.62	0.65
0.4	0.60	0.71	0.61	0.70
0.6	0.61	0.76	0.63	0.71
0.8	0.63	0.80	0.65	0.74

4 Summary and conclusion

We have investigated the momentum distribution of nucleons in asymmetric nuclear matter within the framework of the extended Brueckner-Hartree-Fock approximation. The density dependence and isospin-asymmetry dependence of the nucleon momentum distribution have been predicted. The density dependence, as a function of the ratio k/k_F, turns out to be rather weak, in agreement with the results given in Ref. [6－7]. It is shown that as the asymmetry increases, the neutron depletion below its Fermi momentum becomes

smaller, while the proton depletion below its Fermi momentum becomes larger, which implies that at a higher asymmetry, the many-body correlations induced by the nucleon-nucleon interaction becomes stronger on protons and weaker on neutrons. At momentum $k=0$, the occupation probability for the neutron state increases and for the proton state decreases almost linearly as the asymmetry increases. We have also calculated the quasiparticle strength at the Fermi surface. The obtained result of $Z(k_F)=0.64$ is close to the value 0.63 obtained in NIKHEF experiment for P-shell orbits[16] and in good agreement with other experimental data[4, 8].

References:

[1] JEUKENNE J P, LEJEUNE A, MAHAUX C. Phys Rep, 1976, **25**: 83.

[2] MÜTHER H, KNEHR G, POLLS A. Phys Rev, 1995, **C52**(6): 2955.

[3] SARTOR R, MAHAUX C. Phys Rev, 1980, **C21**: 1546.

[4] BALDO M, BOMBACI I, GIANSIRACUSA G, *et al*. Phys Rev, 1990, **C41**(4): 1748.

[5] JAMINON M, MAHAUX C. Phys Rev, 1990, **C41**(2): 697.

[6] BALDO M, BOMBACI I, GIANSIRACUSA G, *et al*. Nuclear Physics, 1991, **A530**: 135.

[7] ARNAU R, POLLS A, DICKHOFF W. Phys Rev, 2009, **C79**: 064308.

[8] VONDERFECHT B, DICKHOFF W, POLLS A, *et al*. Phys Rev, 1991, **C44**: R1265.

[9] RILEY L, ADRICH P, BAUGHER T, *et al*. Phys Rev, 2008, **C78**: 011303(R).

[10] HA K, AREZKI I, ANDREY T, *et al*. Phys Rev Lett, 2010, **105**: 086403.

[11] FANTONI S, PANDHARIPANDE R V. Nucl Phys, 1984, **A427**: 473.

[12] ZUO W, BOMBACI I, LOMBARDO U. Phys Rev, 1999, **C60**: 024605.

[13] WIRINGA R, STOKS V, SCHIAVILLA R. Phys Rev, 1995, **C51**: 38.

[14] BALDO M, BOMBACI I, GIANSIRACUSA G, *et al*. Phys Rev, 1989, **C40**: R491.

[15] MAHAUX C, SARTOR R. Nuclear Physics, 1993, **A553**(1): 515.

[16] DICKHOFF W, BARBIERI C. Progress in Particle and Nuclear Physics, 2004, **52**: 377.

非对称核物质中核子动量分布的微观理论计算

李建洋[1, 2], 左维[1, 2], 曹高清[1, 2], U. Lombardo[3]

(1. 中国科学院近代物理研究所, 甘肃 兰州 730000;

2. 中国科学院研究生院, 北京 100049;

3. Department of Physics and Astrophysics, Catania University, Via Santa Sofia 64, I-95123, and INFN-LNS, Via Santa Sofia 44, I-95123 Catania, Italy)

摘要: 在 Extended Brueckner-Hartree-Fock(EBHF)近似下, 采用 Argonne V18 势作为核子-核子相互作用, 计算了基态非对称核物质中核子动量的分布。对核子的动量分布对同位旋不对称度的依赖关系进行了描述和讨论。结果表明, 在不对称度为零时, 质子与中子有着基本相同的动量分布。随着不对称度的增加, 在各自的费米面以下, 质子动量分布减小而中子动量分布增大。对费米面处的准粒子强度也进行了计算和讨论。本结果较好地满足了两个理论检验标准 Migdal-Luttinger theorem 和粒子数守恒律。

关键词: 非对称核物质; Brueckner 理论; 动量分布; 准粒子强度

收稿日期: 2011-02-21; **修改日期:** 2011-02-26

基金项目: 国家自然科学基金资助项目(10875151, 10740420550); 中国科学院知识创新工程重大项目(KJCX3-SYW-N2); 国家重点基础研究发展计划项目(2007CB15004); 中国科学院"外国专家特聘研究员"计划(2009J2-26); 中国科学院外国专家局创新团队国际合作伙伴计划

通讯联系人: 左维, E-mail: zuowei@impcas.ac.cn